Determination of F-4 Aircraft Transonic Buffet Characteristics

E. G. Hollingsworth* and M. Cohen†
McDonnell Aircraft Company, St. Louis, Mo.

This paper compares the results of experimental programs conducted to determine the transonic buffet characteristics in several wind tunnels with the results of flight by various techniques on the Model F-4 airplane. Wind-tunnel tests were conducted in cooperation with NASA at Langley Research Center and at McDonnell Douglas wind tunnels. Wind-tunnel instrumentation for buffet onset included a wing tip accelerometer, wing root strain gage, wing trailing-edge pressure taps, and force data. Flight test investigation of buffet characteristics of the Model F-4 airplane was conducted under Air Force Flight Dynamics Laboratory contract. Flight test instrumentation included wing tip and pilots eat accelerometers, wing root, aileron, and stabilator strain gages, wing trailing-edge pressure taps, a boundary-layer pressure rake and wing tufts. Wing leading edge maneuvering slats were also tested in the wind tunnel and in flight in an attempt to improve the maneuvering characteristics of the airplane. Results of buffet data obtained in wind-tunnel and in flight with and without leading edge maneuvering slats are discussed.

Nomenclature

b = span, ft
c = local chord, ft
C = mean geometric chord, ft
C_A = axial force coefficient
C_L = lift coefficient
C_N = normal force coefficient
C_p = pressure coefficient
M = Mach number
PSD = power spectral density
q = dynamic pressure, psf
rms = root mean square
V = velocity, fps
WSG = wing strain gage
WTA = wing tip accelerometer
a_w = wing angle of attack, deg
σ = rms value
ω_1 = first symmetrical wing bending frequency, —Hz
Re = Reynolds number
g = acceleration of gravity, 32.2 fps^2

Introduction

TRANSONIC maneuverability is one of the most important performance parameters of aircraft engaged in air-to-air combat. A complete understanding of buffet characteristic is vital to modern fighter technology and is required to define the buffet phenomenon. It is also essential to determine methods by which wind-tunnel tests can be accomplished which yield buffet onset information close to full-scale flight. McDonnell Aircraft Company has been conducting studies to develop a better understanding of aerodynamic buffet and determine techniques which most consistently predict buffet onset.

This paper reports on an effort to provide better correlation between wind-tunnel and flight test data based on a set of specially installed buffet prediction instrumentation used both in the wind tunnel and in flight on a Model F-4 airplane. This instrumentation included: a wing tip accelerometer, wing root bending moment strain gages, and outer wing static pressure taps. There are three main sections: one each devoted to the methods used, sample results for both the wind-tunnel and flight test studies and, finally, a comparison of wind-tunnel and flight test results.

The flight tests and the wind-tunnel tests conducted at Langley Research Center also investigated improvements in buffet characteristics caused by wing leading-edge maneuvering slats. Correlation of wind-tunnel and flight test results on the slatted airplane are also discussed.

Wind-Tunnel Tests

Wind-tunnel tests were conducted to provide a comparison of the various techniques used in wind-tunnel investigations and to compare with flight buffet boundaries. The wind-tunnel tests were conducted with and without wing leading-edge maneuvering slats at Mach numbers ranging from 0.505–0.94. Four techniques for buffet onset prediction were investigated during these tests. Instrumentation included a wing tip accelerometer, wing strain gage, wing trailing-edge pressure taps, located at 50, 70, 80, and 90% semispan, as well as the standard six component force and moment balance. Figure 1 illustrates the buffet instrumentation and the wing leading-edge slat installation.

The model tested during these programs was a 5% scale model of the F-4E airplane. All structural components of the model were constructed of steel with some brass and fiberglass fairings. Particular care was taken to ensure that the steel wings were rigidly attached to the fuselage to minimize structural damping. Prior to the tests, the wing was oscillated to ensure that the location of the wing bending gages and accelerometer was suitable for measuring the wing fundamental frequencies. Milled pockets and wire channels were incorporated into the wing for the purpose of installing the wing strain gage, wing tip accelerometer, and trailing edge pressure taps. The recesses were filled over the gages, accelerometer, pressure tubes and wires, and the filling was faired to the contour of the wing surface. The wiring and tubing were routed internally through the model into the balance chamber.

The test technique used at the Langley high-speed 7 × 10 ft wind tunnel and at the MCAIR, St. Louis, 4 × 4 ft polysonic wind tunnel for buffet investigation is one developed by Ray and Taylor.[5] The Langley tunnel is a continuous flow facility and had a closed test section for this study. Both the MCAIR polysonic tunnel and the MDC (Calif.) 4 × 4 ft tri-

Presented as Paper 70-584 at the AIAA 5th Aerodynamic Testing Conference, Tullahoma, Tenn., May 18–20, 1970; submitted June 2, 1970; revision received July 13, 1971.
Index category: Aircraft Testing; Subsonic and Transonic Flow; and Aircraft Performance.
* Senior Engineer, Aerodynamics.
† Engineer, Aerodynamics.

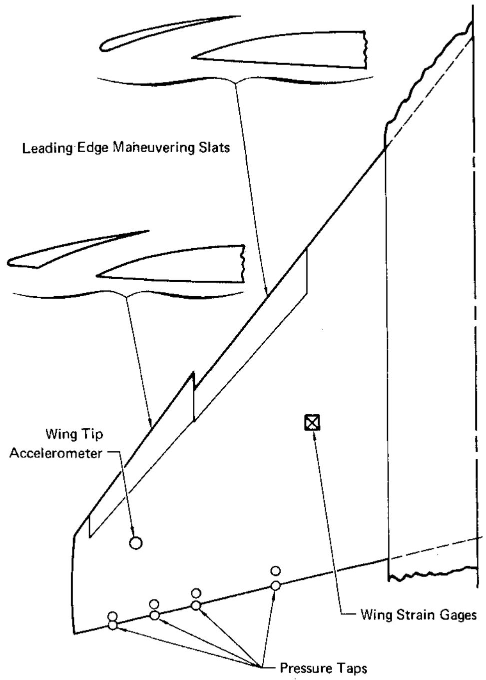

Fig. 1 Wing buffet instrumentation location.

sonic wind tunnel are blowdown facilities with transonic perforated wall test sections. The Mach numbers, Reynolds number, and dynamic pressure for each tunnel are listed in Table 1. Figure 2 illustrates the systematic method of acquiring the data used in buffet onset evaluation. Power-spectra-density and rms values were acquired for both the wing strain gage and wing tip accelerometers over a 45 sec period at each angle of attack in the Langley tunnel. This period was determined from a previous study[5] to be a realistic integration time with respect to available test time and repeatability of the buffet results. In the MCAIR blowdown tunnel, acquisition of the wing strain gage and wing tip accelerometer data was limited to a 30 sec period at each angle of attack because of the relatively short run time common to

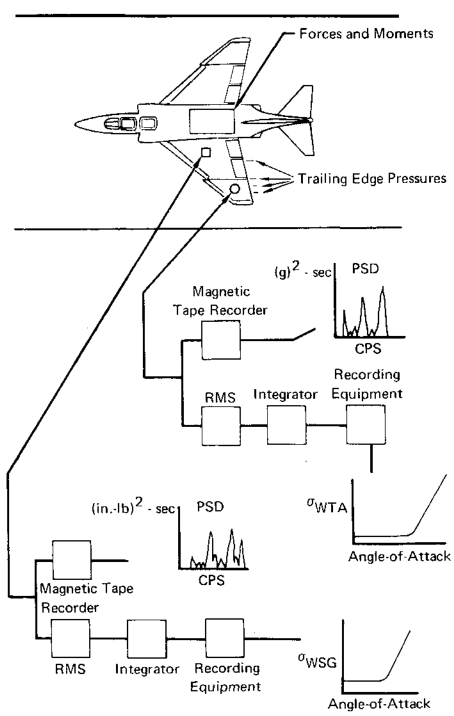

Fig. 2 Wind-tunnel buffet data acquisition.

Table 1 Wind-tunnel parameters

M	q-lb/ft^2	Rn/ft $\times 10^6$
Langley high speed 7 × 10 ft wind tunnel		
0.60	415	3.40
0.70	520	3.70
0.80	620	3.80
0.90	710	3.93
0.94	730	3.65
MCAIR (St. Louis) 4 × 4 ft polysonic wind tunnel		
0.60	882	6.98
0.80	1142	7.24
0.90	1303	7.63
MDC (Calif.) 4 × 4 ft trisonic wind tunnel		
0.50	720	5.85
0.69	1060	7.60
0.73	1180	7.85
0.80	1142	7.24
0.85	1240	7.50
0.90	1303	7.63
0.94	1410	7.80

a blowdown facility. The first 10 sec of the data were not integrated to eliminate any transient effects that may be caused by starting the wind tunnel. Although the results from the wing tip accelerometer were encouraging, the results from the wing strain gage were not. An unknown frequency very close to the first symmetrical bending frequency of the wing prohibited a clear interpretation of the buffet onset from wing strain gage data. Limited tunnel test time prohibited any further investigation into the problem; therefore, the results from the WSG are rated as poor. It is believed that the problem could have been solved either by "retuning" the wing frequency, determining the unknown frequency and changing it if possible, and/or using a narrow band filter in the data reduction.

Table 2 presents a summary of the types of buffet data obtained in all three tunnels. The test program conducted in the MDC (Calif.) trisonic wind tunnel was not a direct part of the buffet study; therefore, no wing strain gage or wing tip accelerometer data were obtained. It can be seen that we have the opportunity not only to compare several techniques for buffet onset prediction but also to compare two types of wind tunnels, a blowdown and a continuous flow type. The wing leading-edge maneuvering slats were tested only in the Langley tunnel.

The rms values of the wing strain gages obtained in the Langley tunnel are presented in Fig. 3 both with and without leading-edge maneuvering slats at $M = 0.8$. The line faired through the data indicates that buffet onset occurs at an angle of attack of 9.5° and 6.7° with and without the wing leading edge slats, respectively. The wing strain gage data indicate a slight rise of σ_{WSG} at low angles of attack before sharp divergence. This slight rise in σ_{WSG} may indicate the

Table 2 Buffet technique investigation summary

	WSG	WTA	Pressure	Force and moment
Without maneuvering slats				
Langley	good	good	fair	good
MCAIR (St. Louis)	poor	good	...	good
MDC (Calif.)	...	...	good	good
With maneuvering slats				
Langley	good	good	fair	good
MCAIR (St. Louis)	...	...	...	...
MDC (Calif.)	...	...	...	...

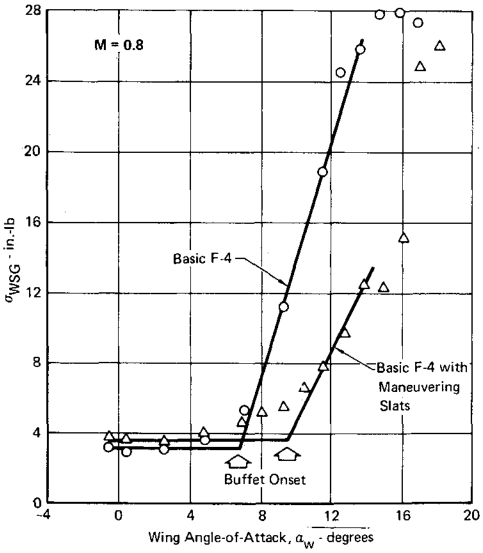

Fig. 3 Wing strain gage, Langley tunnel.

beginning of separation at wing tip followed by the separation moving inboard with an increasing angle of attack demonstrated by the sharp divergence in σ_{WSG}.

The rms values of the wing tip accelerometer obtained in the MCAIR polysonic tunnel are presented in Fig. 4 for the basic F-4 at $M = 0.8$. The fairing indicated buffet onset occurs at an angle of attack of 6.4°.

Wing trailing-edge pressures obtained in the MDC trisonic tunnel at the wing trailing edge and at 95% chord upper surface are presented in Figs. 5 and 6 for the F-4 at $M = 0.8$. The break in the pressure curve signifies airflow separation at the wing surface. The first point of separation occurs at 90% of semispan at about 4°. Data from the stations further inboard indicate separation occurs at higher angles of attack, from 6°–8°. A study of the pressure data and the σ values from the WSG and the wing tip accelerometer gives a clearer understanding of separation phenomena of the F-4 wing. The slight rise in the σ values before the sharp break appears to denote that the wing tip is separating first, with separation moving inboard as the angle of attack is increased.

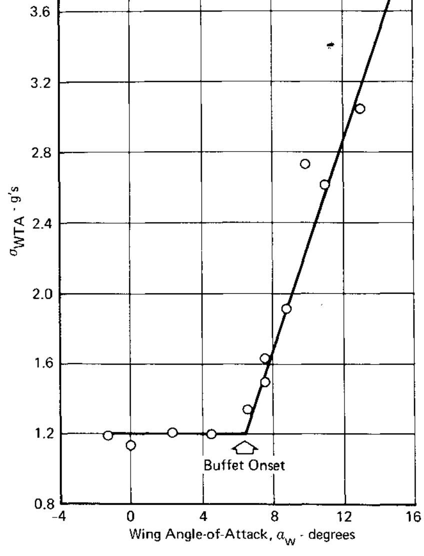

Fig. 4 Wing tip accelerometer, MCAIR polysonic tunnel.

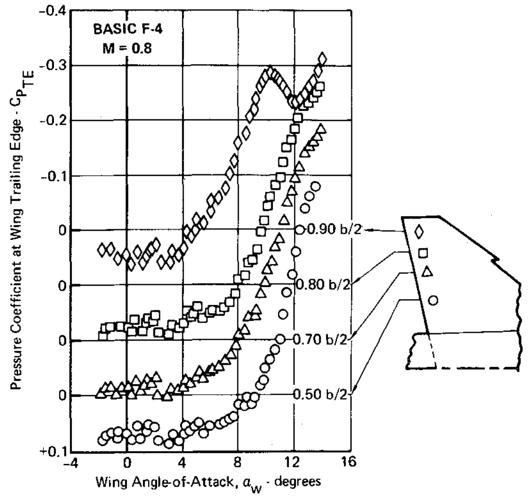

Fig. 5 Pressure coefficient at wing trailing edge, MDC trisonic tunnel.

Figures 7 and 8 present the axial force and lift coefficients both with and without leading-edge maneuvering slats at $M = 0.8$. Buffet onset occurs at 10.6° and 7.0° angles of attack with and without leading-edge slats from the axial force coefficient analysis. Buffet onset was determined to be at the angle of attack at which the wind-tunnel data deviated from a theoretical axial force curve by $C_A = 0.0050$. Buffet onset occurs at 10.1° and 7.2° angles of attack with and without leading-edge slats from the lift curve break analysis.

A summary of the buffet onset data obtained in the wind-tunnels on the F-4 model is presented in Fig. 9. The wind tunnel and technique used to determine buffet onset are indicated in the figure both with and without wing leading-edge maneuvering slats.

Flight Test Program

The purpose of the flight test investigation was to study the buffet characteristics of the F-4 airplane in the transonic flight regime and to determine the effects of wing leading and trailing-edge flap deflection on these characteristics. This effort, under Air Force contract, is documented in Ref. 6. Since the test airplane was utilized previous to this study for evaluation of wing leading edge maneuvering slats by a joint Air Force-Navy Team,[7] it was decided to evaluate the maneuvering slats also during this study. The flight regime included Mach number 0.8–0.9 at constant altitudes of 25,000 and

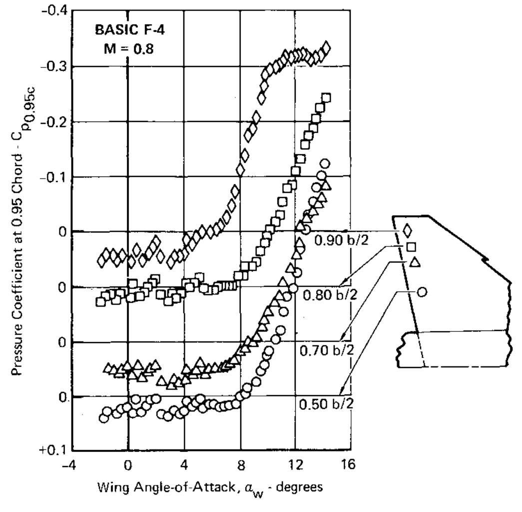

Fig. 6 Pressure coefficient at 0.95 chord, MDC trisonic tunnel.

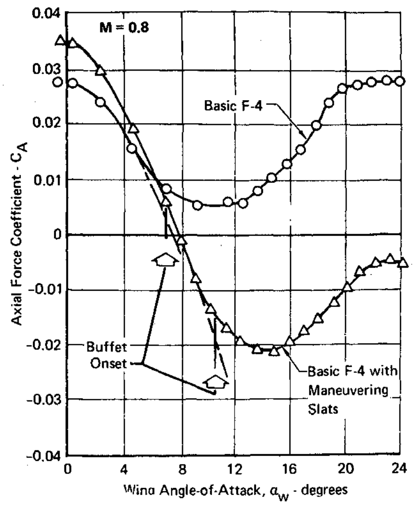

Fig. 7 Axial force characteristics, Langley tunnel.

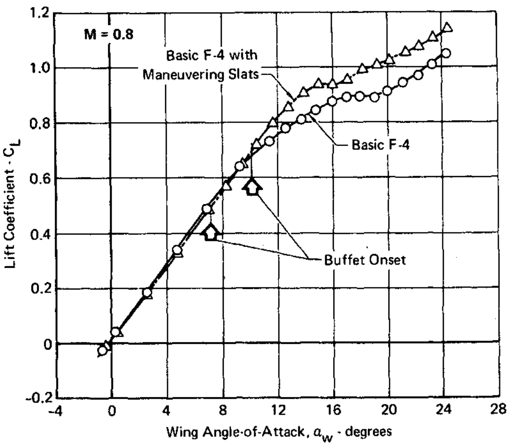

Fig. 8 Lift characteristics, Langley tunnel.

35,000 ft. Wind-up-turns were used exclusively to produce the high angles of attack necessary for buffet study. All wind-up-turns were flown to angles of attack higher than where the pilot indicated buffet onset.

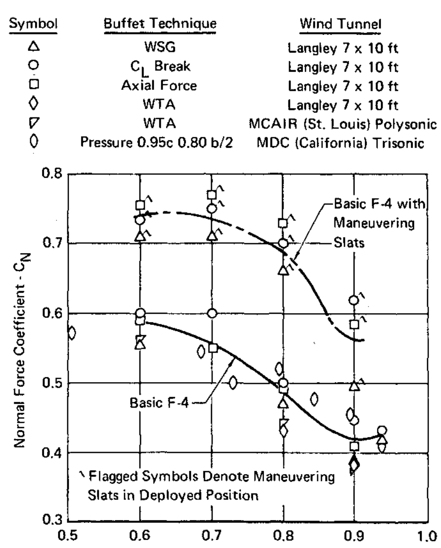

Fig. 9 Summary of buffet onset characteristics of the model F-4 airplane determined from wind-tunnel tests.

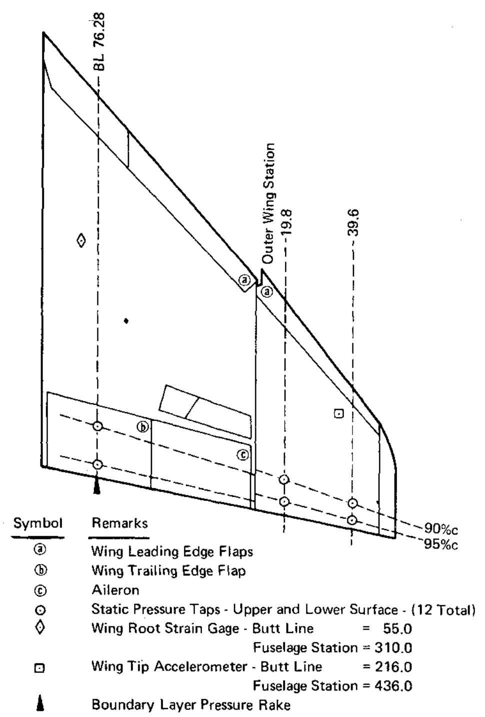

Fig. 10 Model YF-4E, wing buffet instrumentation locations.

A series of specially installed buffet instrumentation was available to study buffet characteristics. This instrumentation included: accelerometers at the wing tip and beneath the pilot seat, strain gages to measure wing root bending moment and aileron and horizontal stabilator actuator rod end axial force, total pressure rake behind the wing trailing edge flap, static pressure taps on the upper and lower wing surfaces, and wing tufts. Both total and static pressure taps were also capable of measuring dynamic response. Location of this instrumentation is shown in Fig. 10.

Data from all instrumentation were examined for the initiation of oscillations which would signify detection of the disturbance caused by airflow separation. The data were subjected to an rms analysis to more accurately determine the point of initial oscillation. In addition, static pressure data, converted to pressure coefficients, were examined for sudden changes which would also signify detection of airflow separation. These indications of airflow separation for each instrument were correlated with pilot indicated buffet onset to determine which type of instrument most accurately could be used to determine buffet onset.

Sample data analysis for the two wing configurations is presented in Figs 11–16. Figure 11 shows the static pressure coefficient data at one altitude and Mach number for the most outboard and most aft static pressure tap on the outer wing panel, Fig. 10. It can be seen that the point of instrumentation detection of airflow separation occurs at 7.4° angle of attack. Figures 12–16 present the rms data for these two configurations at one Mach number and altitude. It should

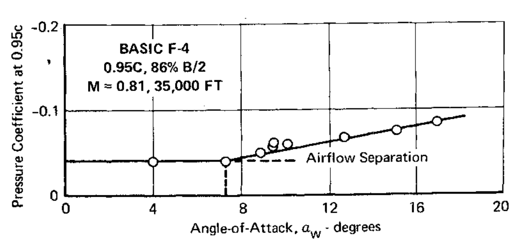

Fig. 11 Model YF-4E, flight test buffet characteristics, instrumentation indication of airflow separation, outer wing static pressure coefficient.

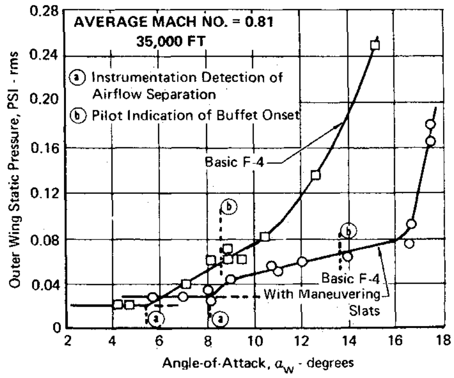

Fig. 12 Model YF-4E flight test buffet characteristics, rms indication of airflow separation, outer wing static pressure, comparison with and without maneuvering slats.

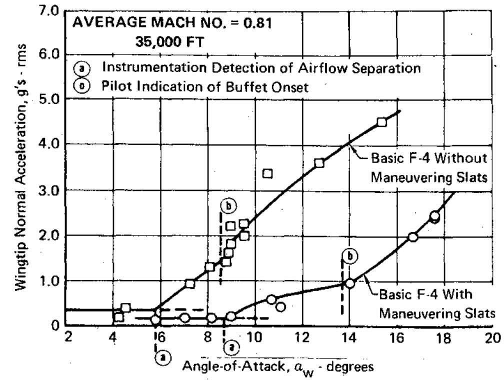

Fig. 14 Model YF-4E flight test buffet characteristics, rms indication of airflow separation, wingtip normal acceleration, comparison with and without maneuvering slats.

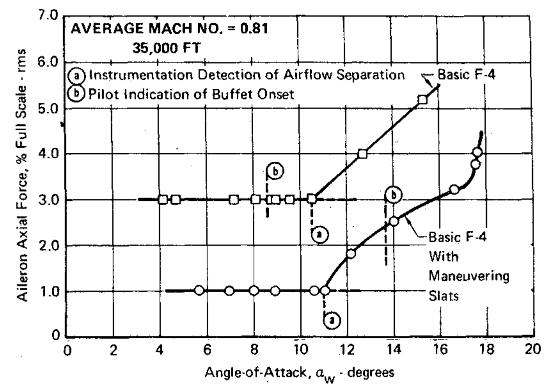

Fig. 15 Model YF-4E flight test buffet characteristics, rms indication of airflow separation, aileron axial force, comparison with and without maneuvering slats.

be noted that all four outer wing upper surface static pressure taps showed evidence of airflow separation (rise in rms level) simultaneously. Therefore, data from only one static pressure tap are shown. This tap was located at the 95% local chord and at approximately 86% semispan; in other words, the most aft and most outboard of those depicted in Fig. 10. Lower wing surface pressure instrumentation gave no evidence of airflow separation, and thus is not included here. All trailing-edge flap instrumentation gave evidence of airflow separation simultaneously. Data obtained from the parameters shown in Figs. 12–16 as well as from the total pressure rake and the static pressure coefficient analysis are summarized as a function of Mach number in Figs. 17 and 18. No significant effects of altitude were found during this investigation.

All pilots flying the maneuvering slat configuration reported a dramatic improvement in buffet characteristics over the clean configuration (all wing flaps undeflected). This improvement consisted of a higher angle of attack for buffet onset, decreased buffet intensities throughout the buffet region and higher maximum attainable load factor. Examination of the rms data in Figs. 12–16 reveals some of the reasons why this improvement occurred. First, maneuvering slats delay initial airflow separation on the outer wing $2\frac{1}{2}°–3°$ angle of attack (wing tip accelerometer and outer wing static pressure). Secondly, the lower intensity of oscillation shown by all parameters also adds to the improvement in pilot indicated buffet onset. This lower intensity of oscillation is due to the fact that, after initial airflow separation, the maneuvering slats slow down the progression of airflow separation across the wing as the angle of attack increases.

As can be seen in Figs. 17 and 18, there is a definite sequence in the angle of attack, independent of wing configuration, where the buffet prediction instrumentation indicated detection of airflow separation. This sequence starts with the wing accelerometer and outer wing static pressure, rms. The next group includes aileron axial force, wing root bending moment, and outer wing static pressure coefficient. This indicates the angle-of-attack region where airflow separation has reached the inner wing. It is interesting to note that the outer wing static pressure rms analysis gave a significantly earlier indication than the outer wing static pressure coefficient analysis. Also, the static pressure rms analysis yielded results much closer to the results obtained from the wing tip accelerometer data. Evidently the rms analysis produces more accurate indications of airflow separation than that possible by analysis of pressure coefficient data. And finally, total pressure at the trailing edge and stabilator axial force gave the final detection of airflow separation. Instrumenta-

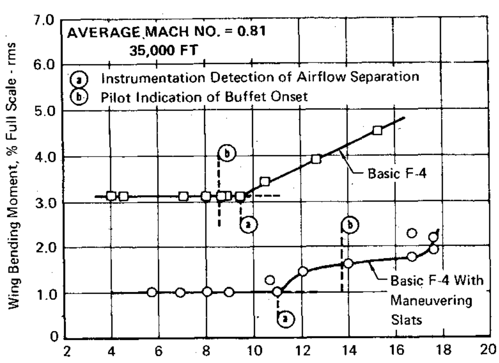

Fig. 13 Model YF-4E flight test buffet characteristics, rms indication of airflow separation, wind bending moment, comparison with and without maneuvering slats.

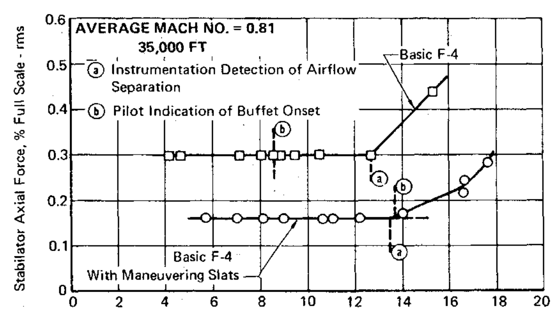

Fig. 16 Model YF-4E flight test buffet characteristics, rms indication of airflow separation, stabilator axial force, comparison with and without maneuvering slats.

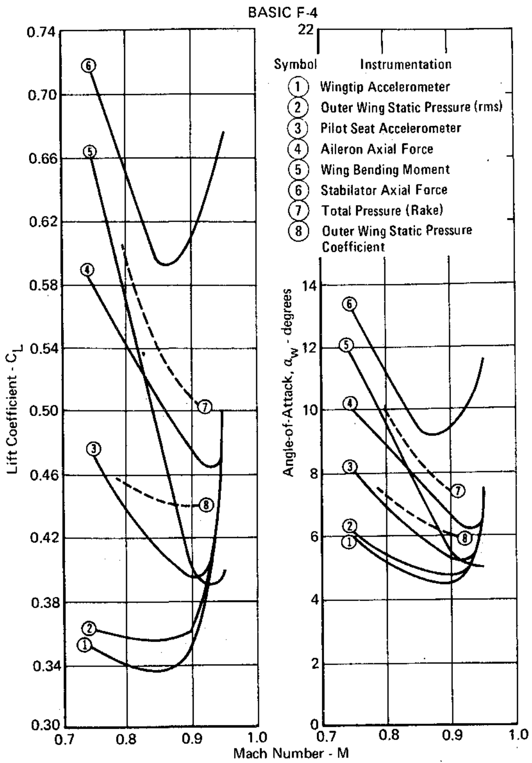

Fig. 17 Model YF-4E flight test buffet characteristics, instrumentation indication of airflow separation.

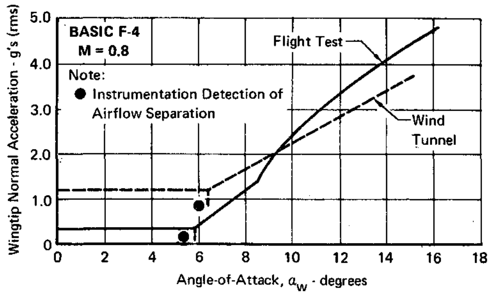

Fig. 19 Wingtip accelerometer, rms indication of airflow separation, comparison of wind-tunnel and flight test results.

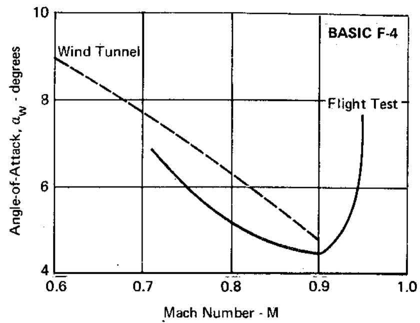

Fig. 20 Wingtip accelerometer, rms indication of airflow separation, comparison of wind-tunnel and flight test results.

tion on the trailing-edge flap and the stabilator is of only limited usefulness because of the very late, high angle of attack detection of airflow separation.

The pilot seat accelerometer gave indication of detection of airflow separation generally at angles of attack between those of the inner and outer wing instrumentation, but displayed some variation within the sequence mentioned above. In all cases the pilot seat accelerometer detected airflow separation at a lower angle of attack than the wing root bending moment. Previous to this test it was thought the opposite would occur since it was reasoned that the disturbance would have to reach the inner wing first and then be transmitted through the fuselage to the pilot seat. Reasons for this phenomenon are not readily apparent and will require further study.

As a result of this study it was determined that the underwing and wing trailing-edge flap pressure taps and horizontal stabilizer actuator axial force can be eliminated from further tests of the Model F-4 airplane. Also, the wing tip accelerometer gave the most accurate and easily determined indication of initial airflow separation of all the instrumentation employed for this test.

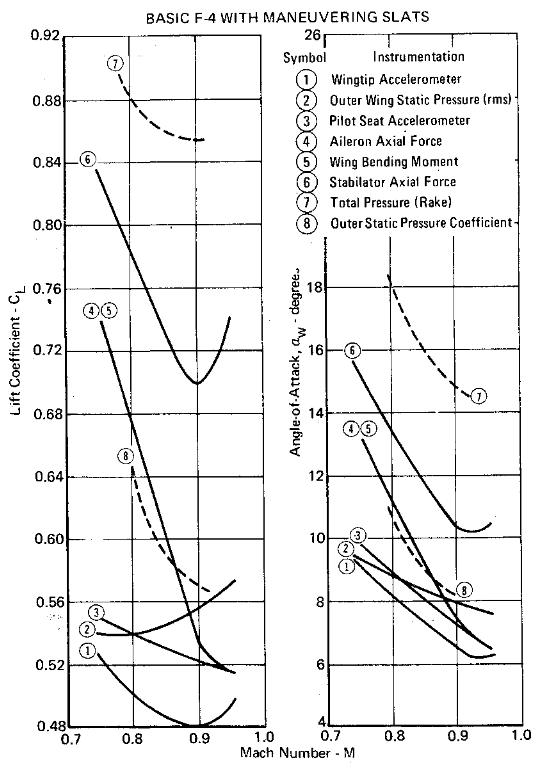

Fig. 18 Model YF-4E flight test buffet characteristics, instrumentation indication of airflow separation.

Wind-Tunnel—Flight Test Comparison

Three buffet techniques were directly comparable from wind tunnel to flight test. The wing tip accelerometer, the outer wing static pressure coefficient and the wing strain gage data were available for wind-tunnel flight test comparison on the basic F-4 airplane. In addition, the wing strain gage data were available for wind-tunnel flight test comparison with the wing leading-edge maneuvering slats in the deployed position on the F-4 airplane. Figure 19 presents the results of the rms indication of airflow separation from the wing tip accelerometer at $M = 0.8$ for the basic F-4. Detection of the

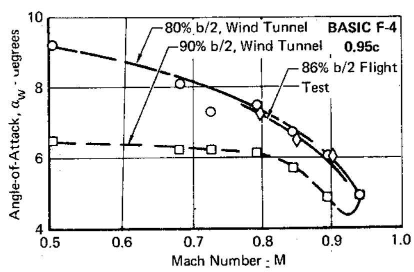

Fig. 21 Outer wing static pressure coefficient, indication of airflow separation, comparison of wind tunnel and flight test results.

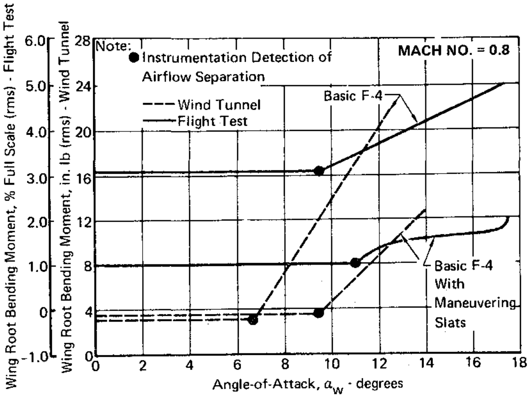

Fig. 22 Wing root bending moment, rms indication of airflow separation, comparison of wind tunnel and flight test results, comparison with and without maneuvering slats.

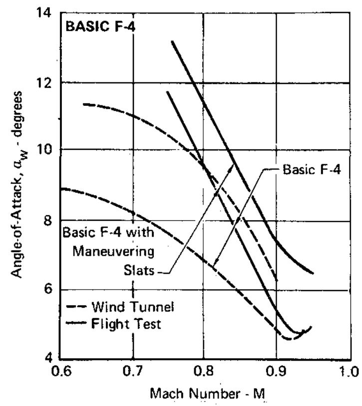

Fig. 23 Wing root bending moment, rms indication of airflow separation, comparison with wind-tunnel and flight test results, comparison with and without maneuvering slats.

point of airflow separation, determined as the initial rise in the rms value of wing tip acceleration, is primarily that which can be determined and compared wind tunnel to flight test. Figure 20 presents a wing tip accelerometer summary as a function of Mach number and wing angle of attack. It can be seen that a close correlation between wind-tunnel and flight test results has been shown. Figure 21 shows similar results of outer wing static pressure coefficients at 95% chord on the wing upper surface. The spanwise location of the pressure taps was not exactly the same, the flight test being at 86% of semispan and the wind tunnel being at 80 and 90% of semispan. It can be seen, as previously discussed, that the 90% semispan data indicate that the extreme outer portion of the wing is separating at a lower angle of attack than the inner portion of the wing. However, excellent agreement for airflow separation is seen for the 86% semispan data from flight test and the 80% semispan data from the wind tunnel. Figures 22 and 23 summarize the results of the wing strain gage data both with and without wing leading edge maneuvering slats. At the lower Mach number shown, the wind-tunnel data indicate airflow separation at a lower angle of attack than flight test data. As the Mach number is increased, good agreement is seen between wind tunnel and flight test.

Conclusions

Good correlation between wind-tunnel and flight test data was obtained for the wing tip accelerometer and outer wing static pressure coefficients in terms of detecting airflow separation. From the standpoint of determining initial airflow separation, the wing tip accelerometer seems best. Static pressure taps are useful in locating the point of initial airflow separation. Wing strain gages are valuable at higher subsonic Mach numbers, but may be misleading at the lower subsonic Mach numbers. It is recommended further flight tests be conducted with wing strain gages to confirm or deny their usefulness as a measure of flight test buffet characteristics. The conclusions of this paper apply mainly to the Model F-4 airplane; however, the relative merits of the buffet instrumentation determined during this study should have general applicability.

References

[1] Mabey, D. G., "Comparison of Seven Wing Buffet Boundaries Measured in Wind Tunnels and in Flight," CP-840, Sept. 1964, British Aeronautical Research Council, London, England.

[2] Mabey, D. G., "Measurements of Wing Buffeting on a Scimitar Model," CP-954, May 1966, British Aeronautical Research Council, London, England.

[3] Seal, D. M., "A Survey of Buffeting Loads," CP-584, 1960, British Aeronautical Research Council, London, England.

[4] Ray, E. J., "Buffet Studies," NASA SP-178, 1968.

[5] Ray, E. J. and Taylor, R. T., "Buffet and Static Aerodynamic Characteristics of a Systematic Series of Wings Determined from a Subsonic Wind-Tunnel Study," TN D-5805, 1970, NASA.

[6] Cohen, M., "Transonic Buffet Characteristics of the Model F-4 Airplane," AFFDL-TR-70-56, April 1970, Air Force Flight Dynamics Lab., Wright-Patterson Air Force Base, Ohio.

[7] Sullivan, D. A., Lt. and Gentry, J. R., Maj., "Final Report, Military Evaluation of the F-4 Wing Leading Edge Slats," FT-119R-69-15, Oct. 1969, Naval Air Test Center, Patuxent River, Md.